In: 2nd International Conference on Cyber-Physical Systems and Control CPS&C, 29 June - 2 July 2021, St. Petersburg, Russia,
Volume 460, Lecture Notes in Networks and Systems, pp. 41-51
DOI: 10.1007/978-3-031-20875-1

Control of Plane Poiseuille Flow Using the Kreiss Constant

Pierre Quénon[1 [0000−0003−4691−5639]] and James F. Whidborne[1 [0000−0002−6310−8946]]

Centre for Aeronautics, Cranfield University, Cranfield, UK
pierre.s.quenon@cranfield.ac.uk
j.f.whidborne@cranfield.ac.uk

Abstract. This paper examines the effectiveness of a recent method based on Kreiss's constant minimization for designing output-feedback compensators to control instabilities in a laminar plane Poiseuille flow. The flow dynamics are highly non-normal, subsequently small disturbances may be substantially amplified and reach large transient values that induce nonlinearities and lead to turbulence, even though such perturbations should eventually decay in a linear flow model. The maximum transient energy growth and the Kreiss constant both convey information regarding this transient behaviour. A Kreiss-constant-minimizing controller is obtained and its effectiveness for the plane Poiseuille flow control problem is demonstrated.

Keywords: Flow Control · Poiseuille Flow · Kreiss Constant · Transient Energy Growth.

1 Introduction

Although Hagen first mentioned flows stability in 1839 and demonstrated it experimentally in 1854, assessing hydrodynamic stability is still recognised as one of the most challenging problems to solve [5]. The transition from laminar to turbulent flow is not fully understood yet but appears to be related to the presence of kinetic energy disturbances and their large transient amplification. In the classical approach, the fluid flow dynamics is linearised about the laminar solution and stability assessed by investigating unstable eigenvalues in the linearised problem. However, this stability criterion may apply only for state-trajectories contained in a small neighbourhood of the laminar solution, and unfortunately, many fluid flow dynamics happen to be highly non-normal. Hence, small perturbations may grow large by a linear mechanism until they are swept away by non-linearities that lead to turbulence, even though such perturbations were expected to decay according to the linear model [14]. As a consequence, predictions made using eigenvalues analysis fail to match most experiments, notably for flows driven by shear forces such as the Couette flow or the laminar plane Poiseuille flow. Eigenvalues analysis for the latter predicts a critical Reynolds number $R = 5772$ at which stability should first occur [10], but the transition to

turbulence is observed experimentally at Reynolds numbers as low as $R \approx 1000$ [4].

This gap between theoretical predictions and experimental results has lead to the development of new approaches for assessing stability. One of those, based on the premise that a flow is unstable only if the energy of the disturbance increases with time, introduces the *maximum transient energy growth*. This quantity conveys the transient amplification behaviour of flows and has proved to be a suitable performance criterion for flows control, and notably for the problem of controlling plane Poiseuille flow. This problem has already drawn considerable attention as reflected in the numerous controller design methods proposed. For instance, [3, 12] and [9] investigates optimal linear quadratic methods and use the maximum transient energy growth in the analysis of the design but not explicitly in the design formulation. A state feedback control that minimizes an upper bound on the maximum transient energy growth has been applied for plane Poiseuille flow [16], but the approach is conservative and state feedback is not available for fluid flow systems. This leads to model-order reduction approches [6]. The maximum transient energy growth output minimization problem problem can be solved by a Q-parametrization [15], but the method is too computationally expensive for the Poiseuille flow problem and results in extremely high order controllers. Another approach based on the method of inequalities has also been proposed in [8] but is again very computationally expensive and suffers from local minima.

However, a new approach based on the minimization of the Kreiss constant for the design of the minimizing transient growth compensator has recently been proposed [2] with better results than the previously mentioned methods on a numerical case study. This method is also a suitable candidate to deal with larger order problems. Here we assess the effectivness of the method to control a linearised model of plane Poiseuille Flow. Section 2 defines the maximum transient energy growth and presents its implication for control. The Kreiss constant design method and the linear plane Poiseuille flow problem are introduced in Sections 3 and 4, respectively. The design results are given in Section 5. Finally, comments and conclusions are provided.

2 Transient Energy Growth

Consider the asymptotically stable linear time-invariant system described by the following Cauchy Problem:

$$\begin{cases} \dot{\underline{x}}(t) = \mathbf{A}\,\underline{x}(t) \\ \underline{x}(0) = \underline{x}_0 \end{cases} \tag{1}$$

where $\mathbf{A} \in \mathbb{R}^{n\times n}$ and $\underline{x}_0 \in \mathbb{R}^n$. The continuous solution for this problem is given by:

$$\begin{array}{rccc} \underline{x}\colon & \mathbb{R}_+ & \longrightarrow & \mathbb{R}^n \\ & t & \longmapsto & \mathbf{e}^{t\mathbf{A}}\,\underline{x}_0 \end{array}$$

The *transient energy growth* $\mathcal{E}(t)$ corresponds to the square of the maximum amplification of a system at time t to all possible initial condition:

$$\mathcal{E}(t) \coloneqq \max_{\|\mathbf{W}\,\underline{x}_0\|=1} \|\mathbf{W}\,\underline{x}(t)\|^2 \;=\; \max \left\|\mathbf{e}^{t\mathbf{A}}\right\|^2 \tag{2}$$

where $\mathbf{W} > 0$ is a constant weighting matrix. In order to obtain information about the maximum amplification of a system to all possible initial conditions at all times, the maximum transient energy growth $\hat{\mathcal{E}}$ is introduced:

$$\hat{\mathcal{E}} \coloneqq \sup_{t\geq 0} \mathcal{E}(t), \tag{3}$$

This definition can be extented to closed-loop systems: consider a linear time-invariant plant transfer function $\mathbf{G}$ with state space:

$$\mathbf{G}(s)\colon \begin{cases} \dot{\underline{x}}(t) = \mathbf{A}\,\underline{x}(t) + \mathbf{B}\,\underline{u}(t) \\ \underline{y}(t) = \mathbf{C}\,\underline{x}(t) \end{cases} \tag{4}$$

where $\mathbf{A} \in \mathbb{R}^{n\times n}$, $\mathbf{B} \in \mathbb{R}^{n\times p}$, $\mathbf{C} \in \mathbb{R}^{m\times n}$ and $\underline{y}(t) \in \mathbb{R}^m$. The plant $\mathbf{G}$ is connected to the dynamical output-feedback controller $\mathbf{K}$:

$$\mathbf{K}(s)\colon \begin{cases} \dot{\underline{x}}_k(t) = \mathbf{A}_k\,\underline{x}_k(t) + \mathbf{B}_k\,\underline{y}(t) \\ \underline{u}(t) = \mathbf{C}_k\,\underline{x}_k(t) + \mathbf{D}_k\,\underline{y}(t) \end{cases} \tag{5}$$

where $\mathbf{A}_k \in \mathbb{R}^{n_k\times n_k}$, $\mathbf{B}_k \in \mathbb{R}^{n_k\times m}$, $\mathbf{C}_k \in \mathbb{R}^{p\times n_k}$, $\mathbf{D}_k \in \mathbb{R}^{p\times m}$ and $\underline{x}_k(t) \in \mathbb{R}^n_k$. The closed loop system is now given by:

$$\begin{cases} \dot{\underline{x}}_{\mathrm{cl}}(t) = \mathbf{A}_{\mathrm{cl}}\,\underline{x}_{\mathrm{cl}}(t) \\ \underline{x}_{\mathrm{cl}}(0) = \underline{x}_{\mathrm{cl}\,0} \end{cases} \tag{6}$$

where

$$\mathbf{A}_{\mathrm{cl}} = \begin{bmatrix} \mathbf{A}+\mathbf{B}\mathbf{D}_k\mathbf{C} & \mathbf{B}\mathbf{C}_k \\ \mathbf{B}_k\mathbf{C} & \mathbf{A}_k \end{bmatrix}, \quad \underline{x}_{\mathrm{cl}}(t) = \begin{bmatrix} \underline{x}(t) \\ \underline{x}_k(t) \end{bmatrix} \quad \text{and} \quad \underline{x}_{\mathrm{cl}\,0} = \begin{bmatrix} \underline{x}_0 \\ \underline{x}_{k\,0} \end{bmatrix}$$

Since only the maximum transient energy growth associated with the plant state needs to be minimised, the transient energy in the controller states is irrelevant to the problem under consideration. Therefore, the matrix $\mathbf{J}$ is introduced for isolating the components of $\underline{x}_{\mathrm{cl}}(t)$ associated to the state of $\mathbf{G}$. The maximum transient energy growth of the closed loop system, concentrated on the plant state trajectories $\underline{x}(t)$ is denoted $\hat{\mathscr{E}}(\mathbf{A}_{cl})$ and is defined as follows:

$$\hat{\mathscr{E}}(\mathbf{A}_{cl}) \coloneqq \sup_{t\geq 0} \|\mathbf{J}^T\,\mathbf{e}^{t\mathbf{A}_{cl}}\mathbf{J}\|^2 \tag{7}$$

where $\mathbf{J} \coloneqq [\mathbf{I}_n, \mathbf{0}]^T$.

The measure $\hat{\mathscr{E}}$ is used as a performance criterion for the controller $\mathbf{K}$ in its process of minimising the transient amplification of the plant $\mathbf{G}$.

3 Plane Poiseuille Flow

Plane Poiseuille flow is steady unidirectional flow between two stationary infinite planes, driven by an externally imposed pressure gradient. Furthermore, no-slip conditions on both bounding planes are assumed. An overview of how a finite state representation for the flow can be derived is presented here, but a more comprehensive description of this derivation can be found in [7]. Consider the Navier-Stokes equations associated to an incompressible steady base flow:

$$\frac{\partial \mathbf{V}_b}{\partial t} + (\mathbf{V}_b \cdot \nabla)\mathbf{V}_b = -\frac{1}{\rho}\nabla P_b + \frac{\mu}{\rho}\nabla^2 \mathbf{V}_b \tag{8}$$

where $\mathbf{V}_b$ is velocity, P_b pressure, ρ is density and μ is viscosity. Because the fluid is assumed to be incompressible and without no sources and sinks, the continuity equation is given by:

$$\rho \nabla \cdot \mathbf{V}_b = 0 \tag{9}$$

The velocity distribution in the fluid has a parabolic streamwise velocity profile with a maximum velocity on the centerline as shown in Fig.1. If small transient flow perturbations $\mathbf{v}, p$ are assumed in the flow, the Navier-Stokes equations can be linearized and converted to a control-theoretic model using a numerical discretization scheme. The linearized non-dimensional Navier-Stokes equations are thus given by:

$$\begin{aligned} \frac{\partial \mathbf{v}}{\partial t} + (\mathbf{V}_b \cdot \nabla)\mathbf{v} + (\mathbf{v} \cdot \nabla)(\mathbf{V}_b + \mathbf{v}) &= -\nabla p + \frac{1}{R}\nabla^2 \mathbf{v} \\ \nabla \cdot \mathbf{v} &= 0 \end{aligned} \tag{10}$$

where R is the dimensionless Reynolds number. Since the state representation of the flow can be obtained using fluid flow field velocity, pressure, and wall shear stresses measurements, and, because the flow can be influenced by manipulations of the conditions on the boundaries (using injection and suction of fluid at the walls as shown for instance in Fig. 1), it is feasible to perform an active feedback control of the evolution of transition in order to prevent perturbations from growing and forming a self-sustaining turbulent flow.

In order to use standard finite-dimension control methods, the equations in (10) are approximated by the following finite-dimension linear time invariant system.

$$\begin{cases} \dot{\underline{x}} &= \mathbf{A}(\alpha, \beta, R)\, \underline{x} + \mathbf{B}(\alpha, \beta, R)\, \underline{u} \\ \underline{y} &= \mathbf{C}(\alpha, \beta, R)\, \underline{x} \end{cases} \tag{11}$$

where the terms α and β are the streamwise and spanwise wave numbers which characterize the spanwise and streamwise boundary conditions. The detailed derivation can be found in [7].

The test case under consideration takes $\alpha = 50$ and $\beta = 52.044$ for $R = 55000$. According to [8], this test case is linearly stable but has the largest transient energy over all unit initial conditions and time and wave-number pairs (α, β), and represents the very earliest stages of the transition to turbulence.

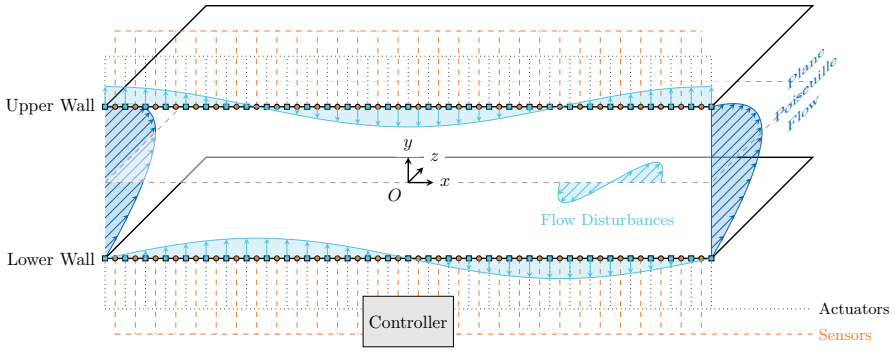

Fig. 1: Plane Poiseuille Flow Control System

4 Transient Energy Minimization Using Kreiss Constant Feedback Control

Consider the asymptotically stable linear time-invariant system (1). The *Kreiss constant* $\mathcal{K}(\mathbf{A})$ of the matrix $\mathbf{A}$ is defined as:

$$\mathcal{K}(\mathbf{A}) \coloneqq \max_{\mathbf{Re}(s)>0} \|(s\mathbf{I}_n - \mathbf{A})^{-1}\|, \tag{12}$$

The importance of this quantity is revealed by its involvement in the bound for $\sqrt{\hat{\mathcal{E}}}$ provided by the *Kreiss Theorem* (see [13], page 183):

$$\mathcal{K}(\mathbf{A}) \leq \sqrt{\hat{\mathcal{E}}} \leq \mathrm{e} \cdot n \cdot (\mathbf{A}). \tag{13}$$

where $n = \dim \mathbf{A}$ and e is Euler's number. Consequently the Kreiss constant is a derived performance criterion for the minimisation of the transient amplification of systems.

A recent method [2] shows that feedback control can be employed to make the Kreiss constant in closed loop significantly smaller. The method takes advantage of the re-expression of the Kreiss constant as a well-known and very convenient H_∞-performance analysis program. Consider the closed-loop system (6). Similarly to how the maximum transient energy growth has been extended to closed-loop systems, [2] introduces the Kreiss constant $\mathcal{K}(\mathbf{A}_{cl})$ of the closed-loop system concentrated on the plant state trajectories:

$$\mathcal{K}(\mathbf{A}_{cl}) \coloneqq \max_{\mathbf{Re}(s)>0} \left\| \mathbf{J}^T \left(s\mathbf{I} - \mathbf{A}_{cl}\right)^{-1} \mathbf{J} \right\| \tag{14}$$

Using the re-expression proposed in [2]:

$$\mathcal{K}(\mathbf{A}_{cl}) = \max_{\delta\in[-1,1]} \|\mathbf{T}^a_{\underline{w}\,\underline{z}}(\delta)\|_\infty = \max_{\delta\in[-1,1]} \|\delta \cdot \mathbf{I} \star \mathbf{P}_a \star \mathbf{K}_a\|_\infty \tag{15}$$

where the worst-case H_∞-norm of $\mathbf{T}^a_{\underline{w}\,\underline{z}}(\delta) \coloneqq \delta \cdot \mathbf{I} \star \mathbf{P}_a \star \mathbf{K}_a$ needs to be determined over parametric uncertainties δ. In order to define explicitly the plant $\mathbf{P}_a$, the augmented system, given by matrices $\mathbf{A}_a$, $\mathbf{B}_a$, $\mathbf{C}_a$ and the augmented state vector $\underline{x}_a \coloneqq \underline{x}_{cl}$ is introduced. The state representation of the augmented system verify $\mathbf{A}_{cl} = \mathbf{A}_a + \mathbf{B}_a \mathbf{K}_a \mathbf{C}_a$, which implies that:

$$\mathbf{A}_a \coloneqq \begin{bmatrix} \mathbf{A} & \mathbf{0} \\ \mathbf{0} & \mathbf{0}_{n_k} \end{bmatrix}, \; \mathbf{B}_a \coloneqq \begin{bmatrix} \mathbf{0} & \mathbf{B} \\ \mathbf{I}_{n_k} & \mathbf{0} \end{bmatrix}, \; \mathbf{C}_a \coloneqq \begin{bmatrix} \mathbf{0} & \mathbf{I}_{n_k} \\ \mathbf{C} & \mathbf{0} \end{bmatrix}, \; \mathbf{K}_a \coloneqq \begin{bmatrix} \mathbf{A}_k & \mathbf{B}_k \\ \mathbf{C}_k & \mathbf{D}_k \end{bmatrix}$$

The plant $\mathbf{P}_a(s)$ can then be defined as:

$$\mathbf{P}_a(s) : \begin{cases} \dot{\underline{x}}_a = (\mathbf{A}_a - \mathbf{I}_{n+n_k})\,\underline{x}_a + \sqrt{2} \cdot \underline{w}_\delta + \mathbf{J}\,\underline{w} + \mathbf{B}_a\,\underline{u} \\ \underline{z}_\delta = -\sqrt{2} \cdot \mathbf{A}_a\,\underline{x}_a - \underline{w}_\delta - \sqrt{2} \cdot \mathbf{B}_a\,\underline{u} \\ \underline{z} = \mathbf{J}^T\,\underline{x}_a \\ \underline{y} = \mathbf{C}_a\,\underline{x}_a \end{cases} \tag{16}$$

$\mathbf{P}_a(s)$ represents the transfer function between ($\underline{w}_\delta$, $\underline{w}$, $\underline{u}$) and ($\underline{z}_\delta$, $\underline{z}$, $\underline{y}$) and is in an upper Linear Fractional Transform (LFT) with the block $\underline{w}_\delta = \delta \cdot \mathbf{I}\,\underline{z}_\delta$, and a lower LFT with the control block $\underline{u} = \mathbf{K}_a\,\underline{y}$. This is represented in Fig. 2, where a gain matrix $\mathbf{Q}$ is introduced for simplifying the block diagram representation :

$$\mathbf{Q} \coloneqq \begin{bmatrix} -\mathbf{I}_n & \sqrt{2} \cdot \mathbf{I}_n \\ -\sqrt{2} \cdot \mathbf{I}_n & \mathbf{I}_n \end{bmatrix}$$

As shown in the Kreiss theorem, synthesizing a controller that minimizes the maximum transient energy growth can be achieved by synthesizing a controller

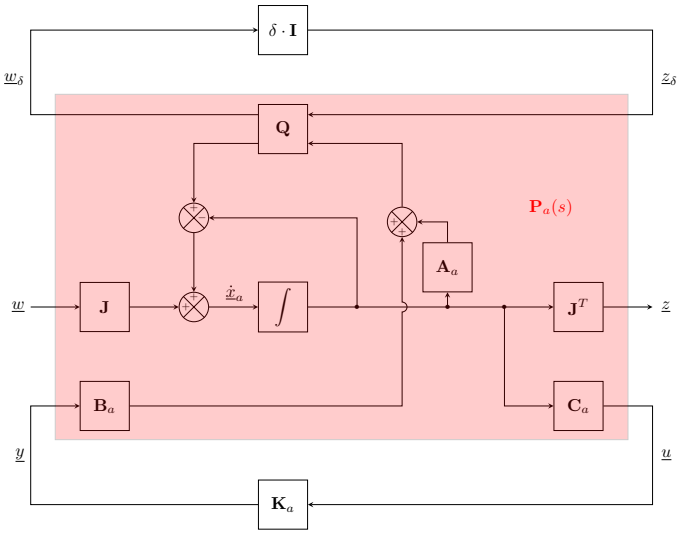

Fig. 2: Block Diagram of Kreiss Constant Re-expression

that minimize $\mathscr{K}(\mathbf{A}_{\mathrm{cl}})$. The latter problem is given by the following program:

$$\begin{aligned} & \min_{\mathbf{K}_a \in \mathbb{K}} \mathscr{K}(\mathbf{A}_{cl}(\mathbf{K}_a)) \\ \iff \quad & \min_{\mathbf{K}_a \in \mathbb{K}} \max_{\delta \in [-1,1]} \|\delta \cdot \mathbf{I} \star \mathbf{P}_a \star \mathbf{K}_a\|_\infty \end{aligned} \tag{17}$$

where $\mathbb{K}$ is a set of controllers with prescribed structure. The program in (17) involves several sources of non-differentiability including the H_∞-norm and the semi-infinite maximum over $\delta \in [-1, 1]$. Solving this program is equivalent to solving an H_∞-parametric robust synthesis problem for the plant $\delta \cdot \mathbf{I} \star \mathbf{P}_a \star \mathbf{K}_a$. An algorithmic approach to tackle this problem, presented in Algorithm 1, has been proposed in [1] and is used in [2]. In order to reduce the computational complexity of the initial problem, Algorithm 1 reduces the large number of scenarios $\delta \in [-1, 1]$ to be considered by operating on a significantly smaller representative set $I \subset [-1, 1]$ that contains dynamically generated parameters associated with problematic scenarios.

Algorithm 1: Parametric Robust Synthesis [2]

Step 1 *Initialization*:
Initialize the bad scenarios set as $I = \{0\}$;

Step 2 *Multi-Model Synthesis*:
Given a finite set $I \subset [-1, 1]$ of scenarios, perform a multi-model H_∞ synthesis

$$h_* = \min_{\mathbf{K}_a \in \mathbb{K}} \max_{\delta \in I} \|\delta \cdot \mathbf{I} \star \mathbf{P}_a \star \mathbf{K}_a\|_\infty$$

and obtain the multi-scenario controller $\mathbf{K}_a^* \in \mathbb{K}$;

Step 3 *Destabilization*:
Compute the worst-case scenario $\delta^* \in [-1, 1]$ by solving

$$\alpha^* = \max_{\delta \in [-1,1]} \alpha(\delta \cdot \mathbf{I} \star \mathbf{P}_a \star \mathbf{K}_a^*)$$

If $\delta \cdot \mathbf{I} \star \mathbf{P}_a \star \mathbf{K}_a^*$ is unstable ($\alpha^* \geq 0$), add δ^* to the bad scenarios set I and go back to **Step 2**. Otherwise ($\alpha^* < 0$) continue ;

Step 4 *Degradation*:
Compute the worst-case performance scenario $\delta^* \in [-1, 1]$ by solving

$$h^* = \max_{\delta \in [-1,1]} \|\delta \cdot \mathbf{I} \star \mathbf{P}_a \star \mathbf{K}_a\|_\infty$$

Step 5 *Termination*:
If $h^* < (1 + tol)\, h_*$, thee degradation is only marginal so accept $\mathbf{K}_a^*$ and continue to **Step 6**. Otherwise add δ^* to the bad scenarios set I and go back to **Step 2** ;

Step 6 *Certification*:
Use a method to certify the final value h^*;

5 Results

5.1 Open-loop

The transient energy $\mathscr{E}(t)$ of the linearized system with no wall transpiration control is shown in Fig. 3. The maximum transient energy growth is $\hat{\mathscr{E}} = 2873.97$.

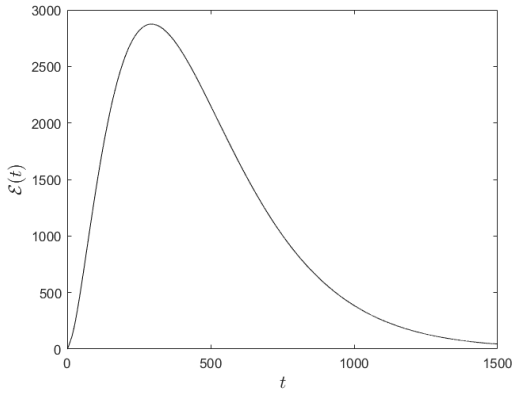

Fig. 3: Transient Energy for Open-loop System

5.2 Kreiss Constant Minimizing Controllers

Algorithm 1 is implemented using MATLAB, and the `HINFSTRUCT` facility used for the H_∞-synthesis in step 2. For the implementation of the global maximum search involved in both steps 3 and 4, the set $[-1, 1]$ is discretized and rough estimates of the local maxima are determined using the MATLAB function `islocalmax`. Precise estimates are then obtained from a bisection search applied on intervals centred on each of the rough estimates. This approach is more naive than the algorithmic solution proposed in [1], but still provides good results and has the advantage of having a low computational burden while guaranteeing a fast convergence to the global maximum α^* and h^*. However, the gain in simplicity is at the expense of poor robustness of the algorithm, which sometimes fails to stabilise the closed-loop system. A more comprehensive description of the implementation process of the algorithm and its limitations can be found in [11].

The program has been tested for computing dynamic controllers of order 2, 3, 4 and 5. The results from the best controllers obtained for 10 restarts are presented in Fig. 4. The explicit definition of thee controllers can be found in [11], Appendix B.

A summary of the results is presented in Table 1. The results show a clear relationship between the controller order and its effectiveness for minimising

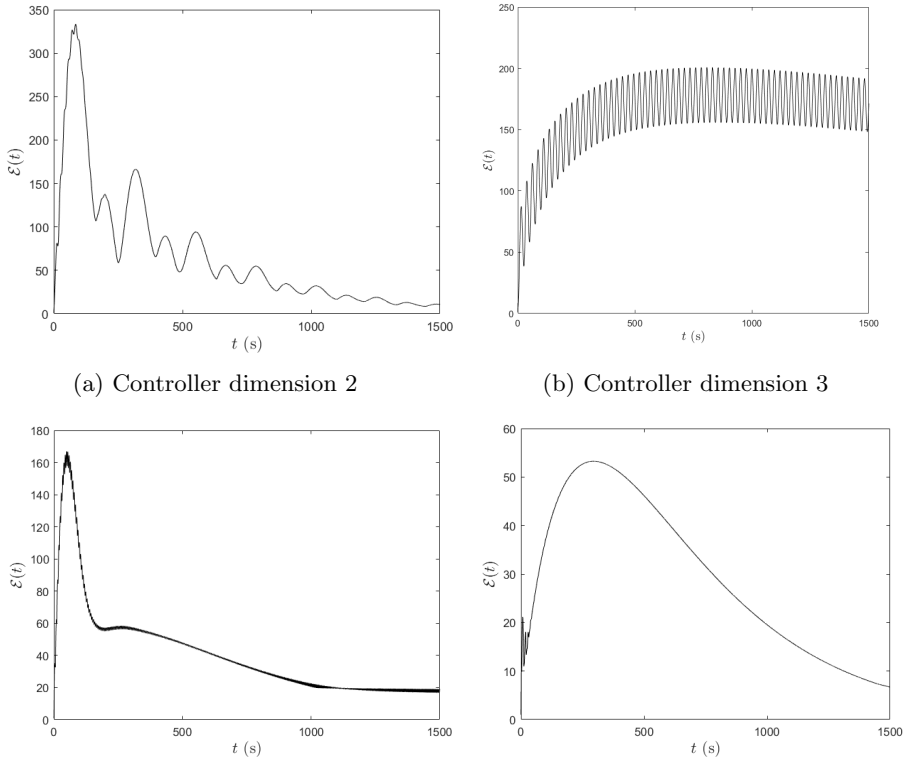

(a) Controller dimension 2

(b) Controller dimension 3

(c) Controller dimension 4

(d) Controller dimension 5

Fig. 4: Transient Energy for Closed-loop System

the maximum transient energy growth: the greater n_k is, the lower $\hat{\mathscr{E}}(\mathbf{A}_{\mathrm{cl}})$ gets. These results exceed those found using competing methods since the best controller (n_k=5) reduces the open-loop maximum transient growth by two orders of magnitude. For comparisons, the approach based on the method of inequalities [8] obtained in the best case $\hat{\mathscr{E}} = 2690.5$ and the approach from [16] to $\hat{\mathscr{E}} = 825$, our results are substantially better with $\hat{\mathscr{E}} = 53.3$. Nonetheless, an unbiased comparison with those previous approaches is difficult since the order of our controllers is significantly greater than the order of controllers found with the competing methods. In particular note that the program returned controllers with impracticable large control gains and low decay rates (see Fig. 4b).

6 Conclusion

In this paper, the design of controllers for plane Poiseuille flow using Kreiss constant minimization has been performed. The best state feedback controller is obtained for $n_k = 5$ with a value of $\hat{\mathscr{E}} = 53,3$. This is considerably lower than the

Table 1: Summary of the Results.

Controller Order n_k	2	3	4	5
$\hat{\mathscr{E}}(\mathbf{A}_{\mathrm{cl}})$	333.3	200.8	155.1	53.3
$\mathscr{K}(\mathbf{A}_{\mathrm{cl}})$	122.49	122.61	122.92	124.35

best value obtained using competing methods. However, the controllers obtained are high order and high gain, and although they lead to low maximum transient energy growth, it is clear that those controllers do not necessarily produce practical control system designs. The aim is not necessarily to synthesise controllers that meet all desired closed-loop specifications but to determine the minimum of the maximum transient energy gain so that designers can judiciously establish specifications for the controller, i.e. to establish a performance benchmark.

Moreover, Algorithm 1 is very sensitive to the algorithm parameter, particularly to the size of the sampling interval involved in the discretization of $[-1, 1]$ in steps 3 and 4. Furthermore, since the starting point used for the optimisation process in step 2 is random and because our algorithm has no guarantee of converging to the optimal solution, our results are hardly repeatable.

A particular difficulty with the implementation of the global maximum searches in step 3 occurs when $\delta \to -1$. The value $\delta = -1$ must be excluded from the search, but the resulting half-open interval can cause numerical difficulties which sometimes lead to the search missing destabilizing peaks and thus to a non-stabilizing controller. A more comprehensive description of those limitations is presented in [11]. Consequently, future investigations of new algorithmic approach for solving program in steps 3 and 4 are necessary to validate the kinds of conclusions that can be drawn from this study for the plane Poiseuille flow. The solutions proposed in [1, sections IV.A and IV.B] might be suitable candidates for further research.

References

1. Apkarian, P., Dao, M., Noll, D.: Parametric robust structured control design. IEEE Transactions on Automatic Control **60**(7), 1857–1869 (2015). https://doi.org/10.1109/TAC.2015.2396644
2. Apkarian, P., Noll, D.: Optimizing the Kreiss constant. SIAM Journal on Control and Optimization **58**(6), 3342–3362 (2020). https://doi.org/10.1137/19M1296215
3. Bewley, T.R., Liu, S.: Optimal and robust control and estimation of linear paths to transition. Journal of Fluid Mechanics **365**, 305–349 (1998). https://doi.org/10.1017/S0022112098001281
4. Carlson, D.R., Widnall, S.E., Peeters, M.F.: A flow-visualization study of transition in plane poiseuille flow. Journal of Fluid Mechanics **121**, 487–505 (1982). https://doi.org/10.1017/S0022112082002006
5. Eckert, M.: The troublesome birth of hydrodynamic stability theory: Sommerfeld and the turbulence problem. The European Physical Journal H **35**(1), 29–51 (2010). https://doi.org/10.1140/epjh/e2010-00003-3

6. Kalur, A., Hemati, M.: Control-oriented model reduction for minimizing transient energy growth in shear flows. AIAA Journal **58**(3), 1034–1045 (2020). https://doi.org/10.2514/1.J058501
7. McKernan, J., Papadakis, G., Whidborne, J.F.: A linear state-space representation of plane Poiseuille flow for control design – a tutorial. International Journal of Modelling, Identification and Control **1**(4), 272–280 (2006). https://doi.org/10.1504/IJMIC.2006.012615
8. McKernan, J., Whidborne, J.F., Papadakis, G.: Design of Poiseuille flow controllers using the method of inequalities. International Journal of Automation and Computing **6**(1), 23–30 (2009). https://doi.org/10.1007/s11633-009-0014-x
9. McKernan, J., Whidborne, J., Papadakis, G.: Linear quadratic control of plane Poiseuille flow - the transient behaviour. International Journal of Control **80**(12), 1912–1930 (2007). https://doi.org/10.1080/00207170701477764
10. Orszag, S.A.: Accurate solution of the Orr–Sommerfeld stability equation. Journal of Fluid Mechanics **50**(4), 689–703 (1971). https://doi.org/10.1017/S0022112071002842
11. Quénon, P.: Design of Flow Controllers Using the Kreiss Constant. M.Sc. thesis, Cranfield University, Bedfordshire, U.K. (2021)
12. Sun, Y., Hemati, M.: Feedback control for transition suppression in direct numerical simulations of channel flow. Energies **12**(21) (2019). https://doi.org/10.3390/en12214127
13. Trefethen, L., Embree, M.: Spectra and Pseudospectra: The Behavior of Nonnormal Matrices and Operators. Princeton University Press (2005). https://doi.org/10.2307/j.ctvzxx9kj
14. Trefethen, L., Trefethen, A., Reddy, S., Driscoll, T.: Hydrodynamic stability without eigenvalues. Science **261**, 578–584 (1993). https://doi.org/10.1126/science.261.5121.578
15. Whidborne, J.F., McKernan, J.: On the minimization of maximum transient energy growth. IEEE Transactions on Automatic Control **52**(9), 1762–1767 (2007). https://doi.org/10.1109/TAC.2007.900854
16. Whidborne, J., McKernan, J., Papadakis, G.: Minimizing transient energy growth in plane Poiseuille flow. Proceedings of the Institution of Mechanical Engineers, Part I: Journal of Systems and Control Engineering **222**(5), 323–331 (2008). https://doi.org/10.1243/09596518JSCE493

Control of plane Poiseuille flow using the Kreiss constant

Quénon, Pierre

2023-01-21

Quenon P, Whidborne JF. (2023) Control of plane Poiseuille flow using the Kreiss constant. In: 2nd International Conference on Cyber-Physical Systems and Control CPS&C, 29 June - 2 July 2021, St. Petersburg, Russia, Volume 460, Lecture Notes in Networks and Systems, Springer, Cham, pp. 41-51

https://doi.org/10.1007/978-3-031-20875-1_5